Space Application for Disaster Monitoring

Collection of Good Practice in Disaster Emergency Observation by ALOS-2 “DAICHI 2” from 2014 to 2017 (Excerpts)

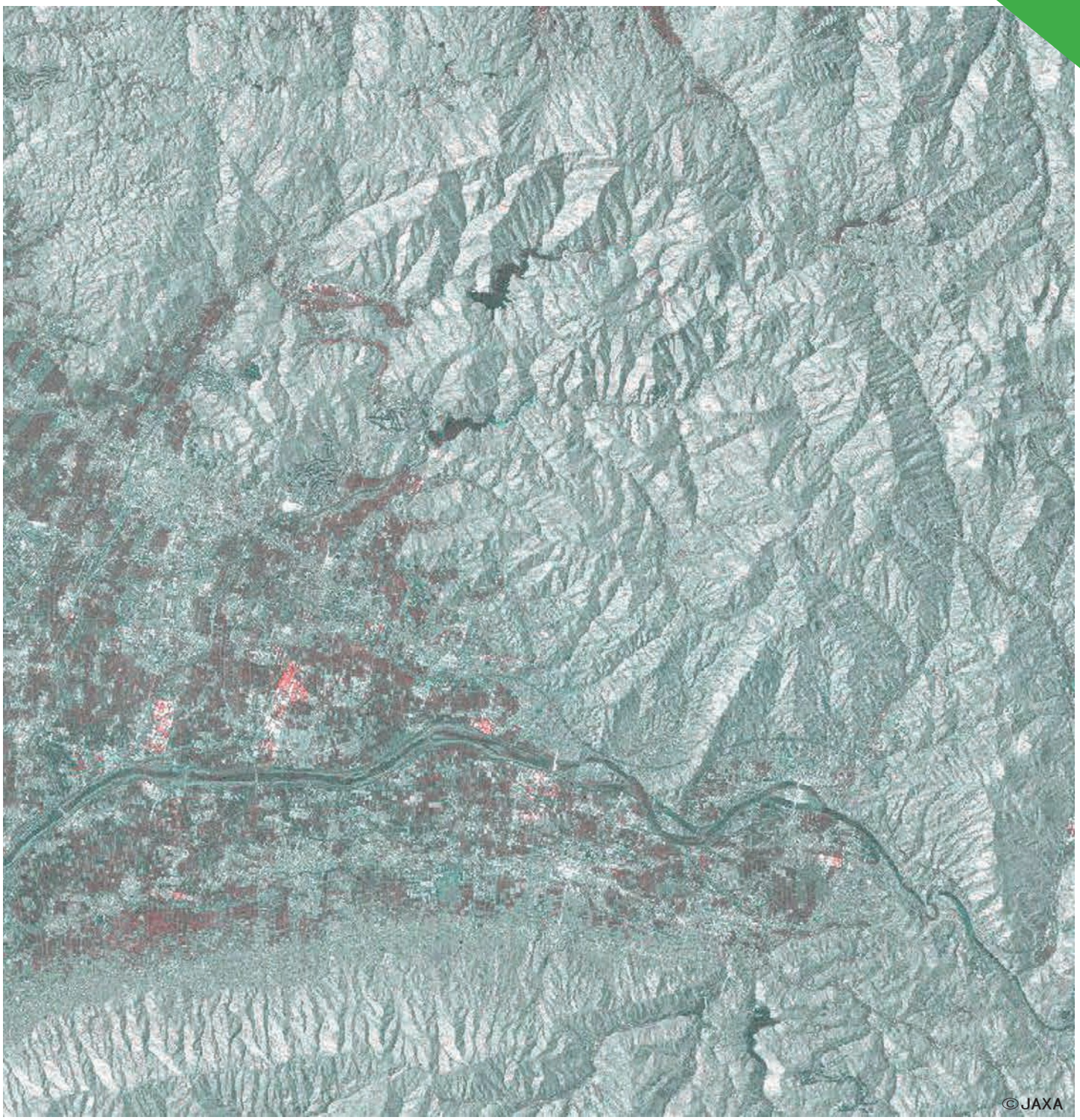

ALOS-2 (Advanced Land Observing Satellite-2)

Overview of ALOS-2

The earth observation satellite ALOS-2"DAICHI-2" was developed as the successor to ALOS "DAICHI". It takes over the mission of DAICHI contributing in various ways to our lives through utilization in mapping, regional observation, disaster monitoring and resource exploration.

DAICHI-2's onboard instrument enhances DAICHI's Phased Array type L-band Synthetic Aperture Radar (PALSAR). Improved performance in aspects such as resolution and regions that can be observed, makes it possible to provide information more accurately and swiftly.

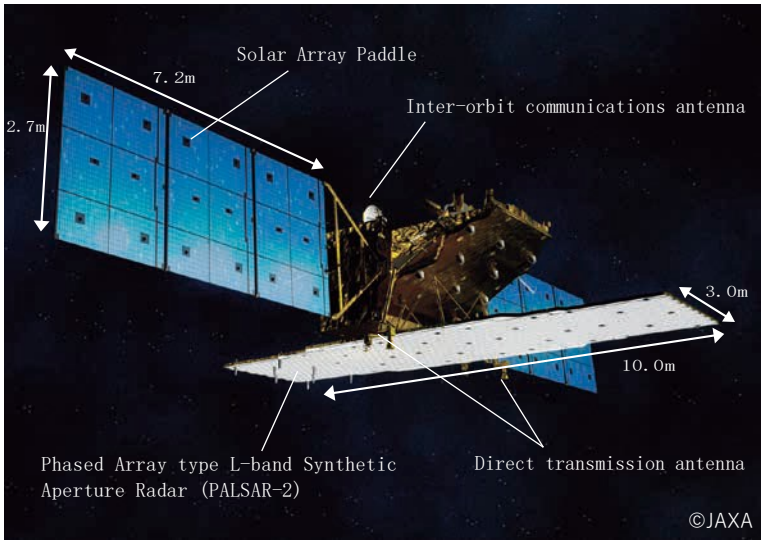

Fig. 1: ALOS-2 in-orbit configuration

Table 1: Main specifications of ALOS-2

Launch	Date	24 May 2014
	Launch vehicle	H-IIA launch vehicle No. 24
Design life		5 years (target: 7 years)
Operational orbit	Type	Sun-synchronous sub-recurrent orbit
	Altitude	628km (above the equator)
	Local sun time at descending node	12:00+/- 15min
	Revisit time	14 days
Satellite size (on orbit)		Approx. 10.0m x 16.5m x 3.7m
Satellite mass		Approx. 2,100 kg
Mission instrument (frequency)		Phased Array type L-band Synthetic Aperture Radar PALSAR-2 (1.2 GHz band)

ALOS-2 also carries the Space-based Automatic Identification System Experiment 2 (SPAISE-2), and the Compact Infrared Camera (CIRC) as technology demonstration missions.

Characteristics of ALOS-2

1 Observation of Wide Areas on the Earth

ALOS-2 satellite body can tilt right and left to observe on both sides. It also uses the phased array method which can swing radar waves (beams) electronically. Thus it is possible to expand its observation range to 2,320 km, almost three times greater than DAICHI's. ScanSAR Mode can achieve 490km swath which is wider than 350km of ALOS/PALSAR.

2 High-resolution Observation Regardless of Day or Night and Weather Conditions

The greatest characteristic of Synthetic Aperture Radar (SAR) is its ability to observe the Earth's surface day and night, regardless of weather conditions. As ALOS-2's PALSAR-2 uses L-band, influence by weather conditions is smaller compared to X-band or C-band used by other satellites. PALSAR-2 also has Spotlight Mode to achieve the resolution of 1m x 3m, allowing it to carry out observations at a higher resolution as compared to ALOS.

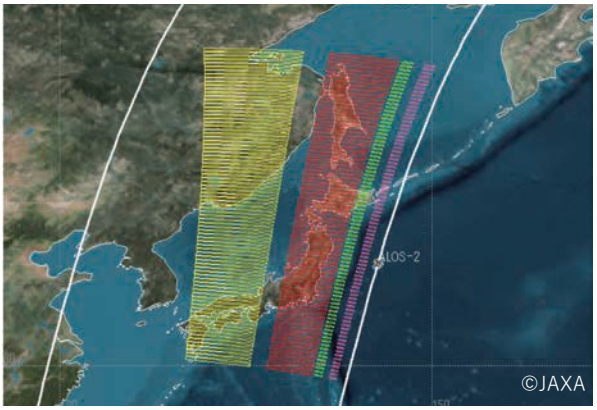

Fig. 2: ALOS-2 observation coverage image

Yellow band: ScanSAR Mode (Swath width: 490km)
Red band: ScanSAR Mode (Swath width: 350km)
Green band: Stripmap (10m) Mode (Swath width: 70km)
Pink band: Stripmap (3m/6m) Mode (Swath width: 50km)

3 Emergency Observation Response to Disasters

ALOS-2 realizes emergency observation by left-and-right looking capability, the significant reduction in revisit time (to target quickly on the location to be observed) and improved data transmission ability. In the case that the emergency observation for natural disaster is required in Japan, images of the disaster area can be obtained in two hours at the minimum. ALOS-2 emergency observation has contributed for Sentinel Asia and International Disaster Charter in mutual collaboration with space agencies etc.

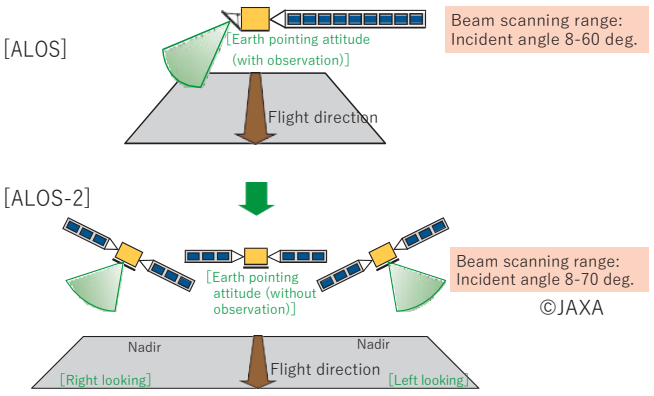

Fig. 3: ALOS-2 observation attitude

Observation Modes

ALOS-2 has three observation modes. We can choose from Spotlight Mode with the resolution of 1m x 3m for the most detailed observation, Stripmap Mode with the resolution of 3-10m (swath width of 50-70km), and ScanSAR Mode to cover a wide area in just one observation (resolution of 60-100m, swath width of 350-490km). It is possible to realize the optimal observation by selecting the most appropriate observation mode according to your objectives.

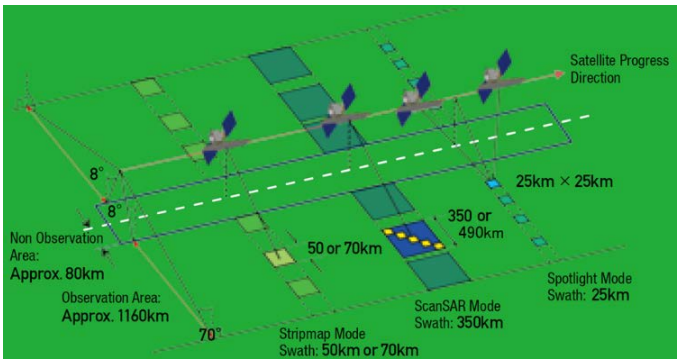

Fig. 4: Illustration of each observation mode

Table 2: List of observation modes

Observation mode	Resolution	Swath
Spotlight	1m (Azimuth) x 3m (Range)	25km (Azimuth) x 25km (Range)
Stripmap	3m	50km
	6m	50km
	10m	70km
ScanSAR	60m	490km
	100m	350km

"Azimuth" means satellite flight direction.
"Range" means range direction in which beam is transmitted (at right angles to azimuth direction).

Spotlight Mode

Adding Spotlight Mode as a new observation mode makes it possible to obtain better quality images at the high resolution of 1m x 3m on ALOS-2. Spotlight Mode enables to increase the illumination time selecting observation areas locally. As a result, it is now possible to capture the Earth's surface in more detail.

Fig. 5: Image captured using Spotlight Mode (around Maihama Station)

Stripmap Mode

Incorporating the dual-beam system into PALSAR-2 makes it possible to maintain a high resolution and wide swath width in Stripmap Mode. Disaster monitoring is conducted mainly using Stripmap Mode.

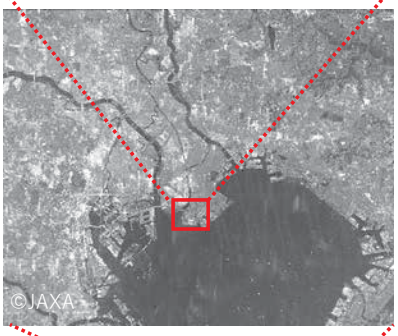

Fig. 6: Image captured using Stripmap Mode (Tokyo, Chiba area)

ScanSAR Mode

ALOS-2 can capture images over an extremely wide area of 350km or 490 km swath. This ScanSAR Mode is utilized to capture crustal deformations caused by massive earthquakes.

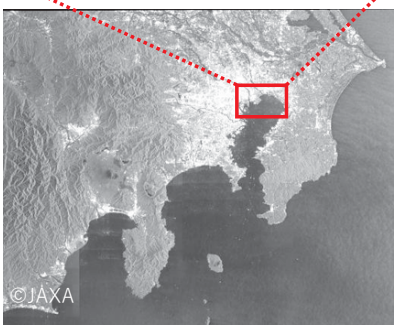

Fig. 7: Image captured using ScanSAR Mode (Kanto region)

Emergency Observation Requests

ALOS-2 passes over Japan twice daily at midday (day pass) and midnight (night pass) JST (with variation range of around 1.5 hours before or after). Emergency observation requests may be received until one hour before command uplink. Automatic analysis for disaster map can be provided within around two hours after observation and disaster affected area information within around five hours after observation for the disaster that occur in Japan.

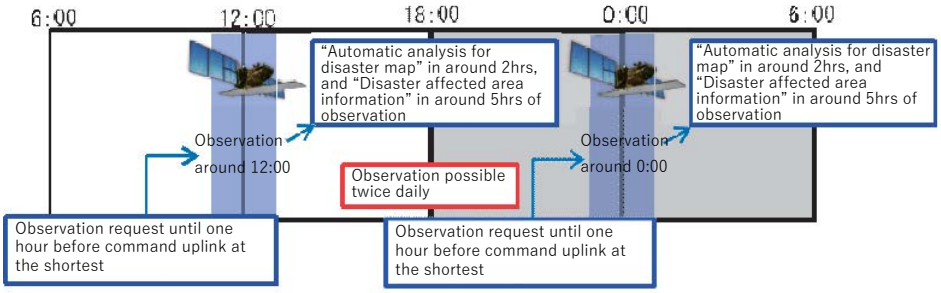

Fig. 8: Observation time schedule

Overview of Image Analysis

Superimposition of images from different timings

SAR is an instrument that emits radio waves towards the observation target and measures the reflected wave returning to the satellite. In general, when the observed target has a smooth surface like water surface, reflected waves are few, and when the surface is rough, the reflected waves increase. Especially when there are many branches and leaves and dense trunks like forests, many reflected waves are generated.

As shown in Fig. 1, the SAR image is obtained by imaging the intensity of the reflected wave, that is, the situation on the ground surface, in shades of black and white. The water surface appears black, and the image becomes whiter as reflected waves increase.

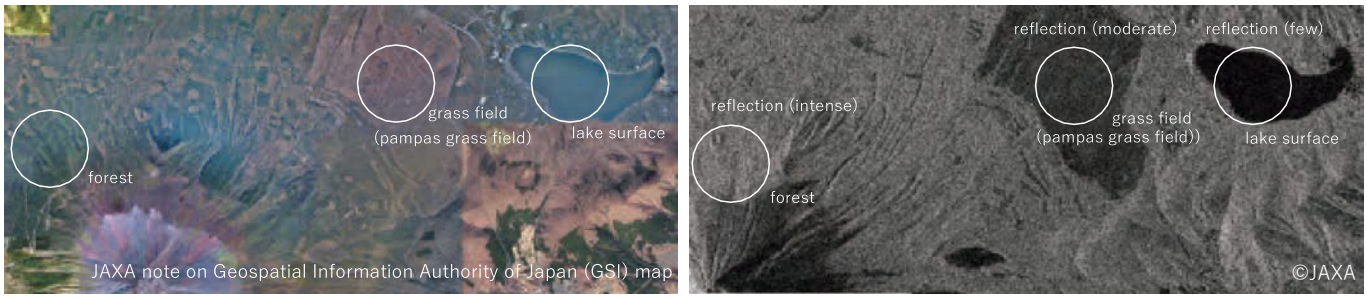

Fig. 1: How SAR image appears (left: aerial photograph, right: SAR image obtained by ALOS-2)

For example, as shown in Fig. 2, the exposed ground before the disaster appears relatively dark on the SAR image, but when the rough surface changes to water surface due to flooding, it appears very dark.

On the other hand, as shown in Fig. 3, in a forest-covered mountainous area, before the landslide, many reflection waves are generated by the forest where the branches and leaves are dense, so it appears bright. But when a part of the forest is lost due to landslide, that area will be replaced by exposed ground with less reflected waves, so it will appear dark. In this way, since the shading on the SAR image changes before and after the disaster, it is possible to estimate the affected area by comparing the two SAR images before and after the disaster.

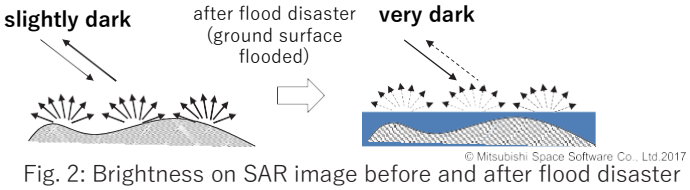

Fig. 2: Brightness on SAR image before and after flood disaster

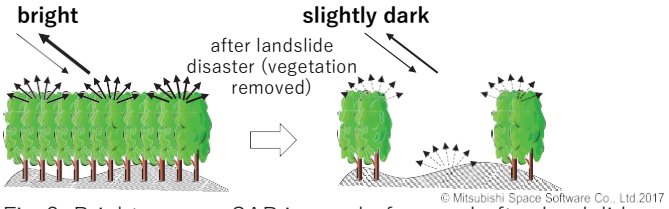

Fig. 3: Brightness on SAR image before and after landslide disaster

When superimposing images before and after the disaster, in order to extract the change before and after the disaster, images from different timings are assigned three colors, red, green and blue respectively, and color composite display is performed.

In Fig. 4, green and blue are allocated to the post-disaster image, and red to the pre-disaster image. You can see the part displayed in red on a part that seems to be flat ground on this image. This is presumed to be because, compared to the pre-disaster earth surface assigned red, the reflected wave from the post-disaster earth surface assigned green and blue is extremely weakened by flooding. Therefore, the red area is extracted as area suspected of flooding damage.

Pre-disaster image expressed in red　　Post-disaster image expressed in green & blue　　Images from two timings superimposed

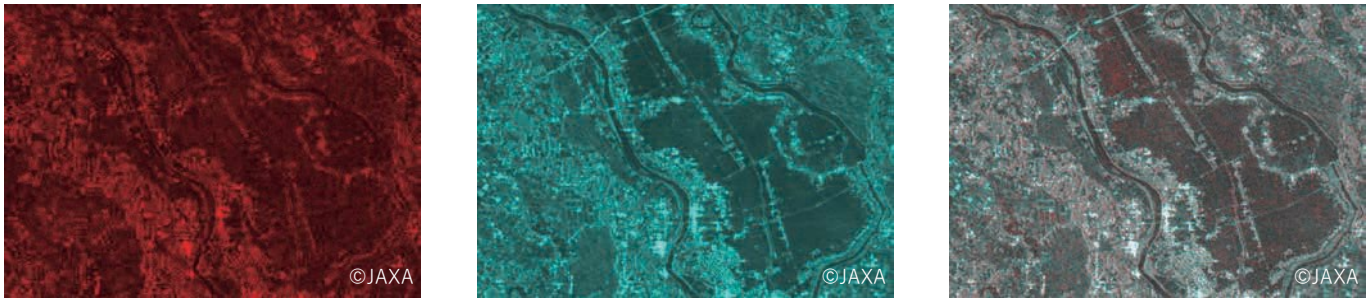

Fig. 4: Enhancement of disaster affected areas by color composite display of images from before and after the disaster

Fig. 5 shows an example of color composite image from two timings taking the case of flood. You can see where the flooded area is spreading in red.

Fig. 6 shows an example of color composite image from two timings taking the case of heavy rain and landslide. Forests are displaced showing exposed soil in the red area, and the area with suspected inflow of soil is extracted in light blue. When conducting analysis by superimposing two images from different timing, as only the change in the object observed is extracted, accuracy of disaster effect extraction can be improved by setting the observation conditions (ascending/descending orbit, off nadir angle etc.) to be the same.

Fig. 5: Example of superimposition of images from two timings (the case of flood)

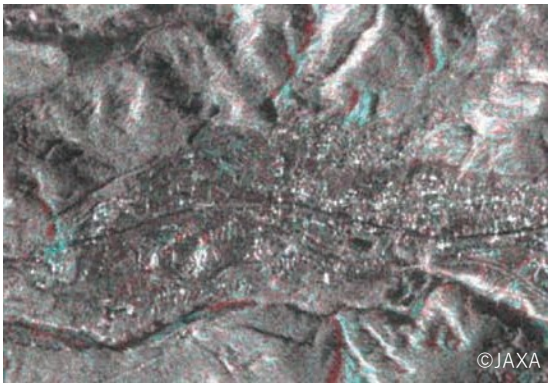

Fig. 6: Example of superimposition of images from two timings (the case of heavy rain and landslide)

Superimposition of images with different polarized waves

Radio waves are transverse waves that vibrate in a plane perpendicular to the direction of travel, and the characteristic of polarization in which wave vibration is enhanced in a specific direction is known. There are types of polarized waves, such as elliptically polarized waves and linearly polarized waves, but when the radio waves are reflected from the object, the characteristics of the polarized wave may change depending on the type of the object to be reflected. In ALOS-2, in order to capture the change in polarization due to the ground object, we observe by switching between linear polarized wave oscillating horizontally (H) and linear polarized wave oscillating vertically (V) at the time of transmission and reception. Fig. 7 shows the combination of polarizations used for observation by ALOS-2. When transmission and reception are both H it is called “HH”, when transmission is H(V) and reception is V(H) it is called “HV”(“VH”), and when transmission and reception are both V it is called “VV”.

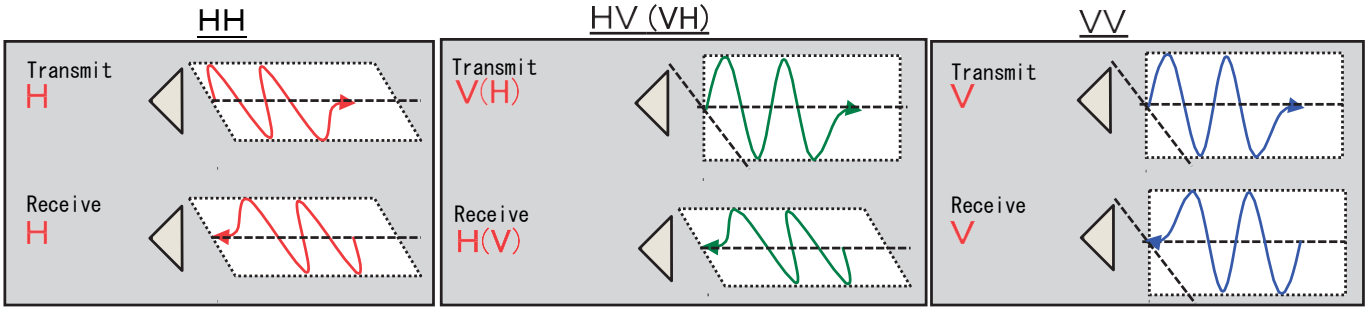

Fig. 7: Polarized wave observation by SAR

Fig. 8 shows an example of observation image using two polarized waves of HH and HV in mountains covered with vegetation. In this example, HH is assigned red and blue, and HV is assigned green, indicating that HV is dominant in most areas. Generally, with L-band SAR, HH is known to show high response to ground structure and bare ground, HV to vegetation such as forest, and VV to bare ground. By switching polarized waves and observing the characteristics of polarized waves by ground objects, it is possible to estimate whether vegetation covers the ground or the ground surface is exposed.

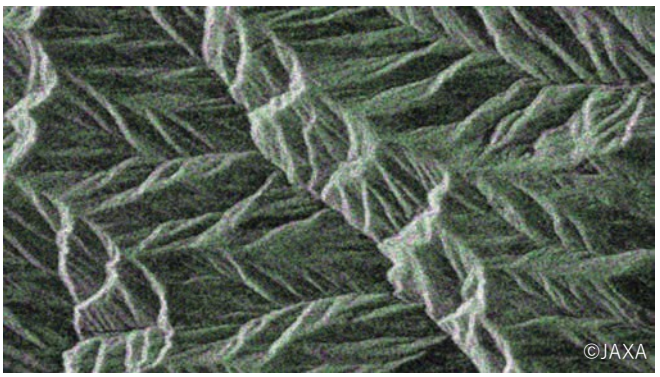

Fig. 8: Example of polarized wave composite image

Interferometric SAR Analysis

Radio waves have the characteristics of waves as their name suggests, and peaks and troughs (the position of a point in time between the two being called a “phase”) are repeated at regular intervals. As Fig. 9 shows, the phase state at reception will not change if the distance the radio wave travels from transmission by the instrument, reflection by the observation target and return to the instrument remains unchanged. If, however, this distance somehow changes, then the phase state at reception will change. For example, when the satellite position does not change and the terrain rises as in Fig. 9, then the distance between that peak and the instrument becomes shorter than before the terrain rise.

Such image obtained by calculating the phase difference obtained from two observations for each pixel on the two-dimensional SAR image is called an "Interferometric SAR image”. In this way, it is possible to capture how much the ground surface rises in the direction of the satellite. On the other hand, when the terrain sinks, the distance between that point and the instrument becomes longer, so the sign of the phase difference will be the reverse of when the ground rises. So, by interferometric SAR analysis, it is possible to distinguish topographical variation both approaching and moving away from the instrument. From this principle, it is possible to extract crustal deformation on the scale of several centimeters by interferometric SAR analysis.

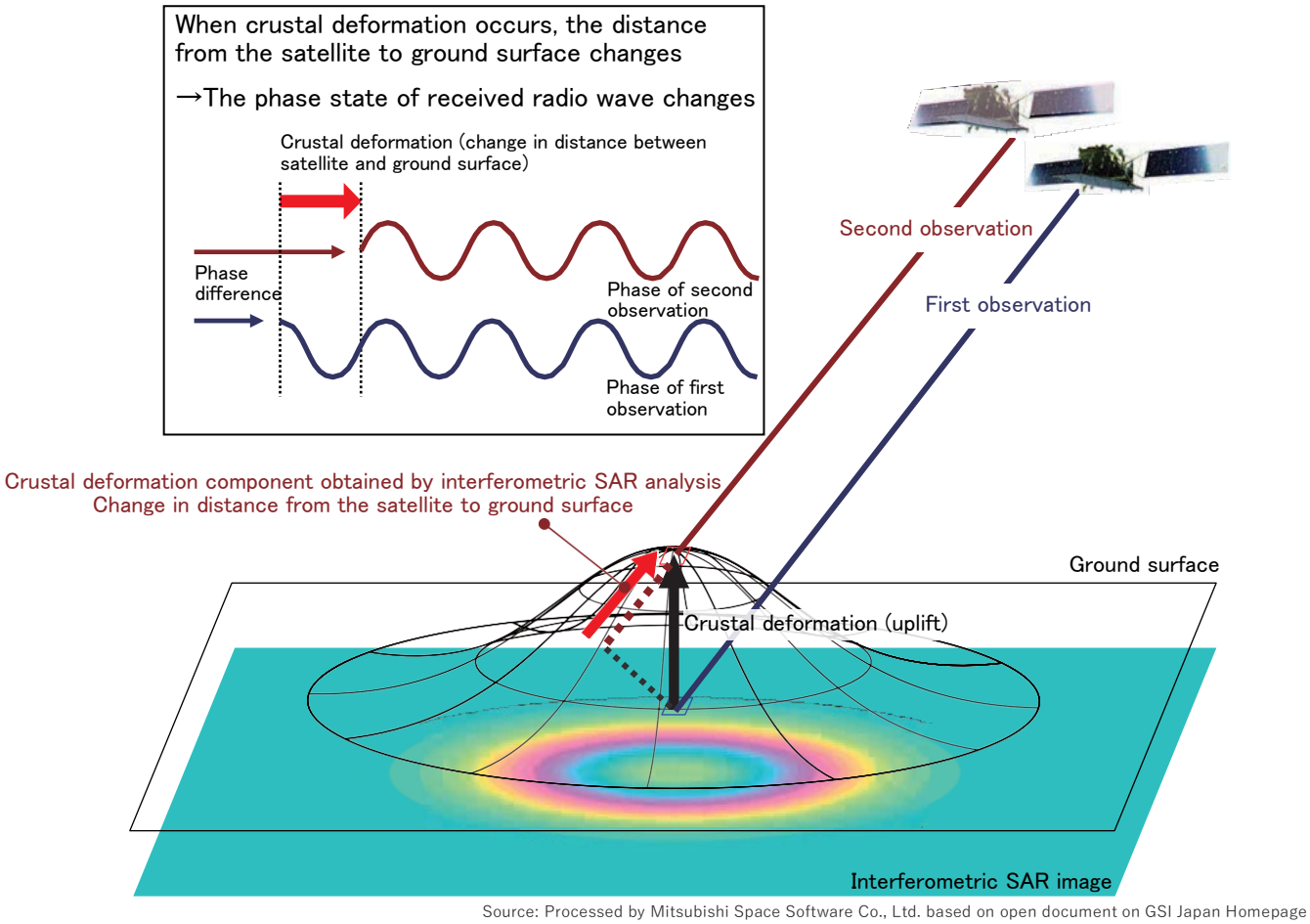

Source: Processed by Mitsubishi Space Software Co., Ltd. based on open document on GSI Japan Homepage

Fig. 9: Schematic diagram of crustal deformation component obtained by interferometric SAR analysis

On the other hand, in two observations, when a certain surface shows a change that moves as a whole, a phase difference occurs before and after fluctuation (interference fringes are generated), but a phase difference between adjacent pixels will not occur. However, for sudden changes that make the ground surface uneven, adjacent phases differ piecemeal, so interference fringes cannot be obtained and terrain change cannot be measured.

The state of the phase difference between adjacent pixels is called coherence. In the former case, the coherence is high and in the latter random case the coherence is low. Coherence is sensitive to abrupt changes such as collapse of ground and buildings due to eruptions and earthquakes, so it is one of the important methods of interferometric SAR analysis for damage situation before and after a disaster.

Image analysis method and examples in this document

The methods of image analysis corresponding to the case of disaster described in this document are as follows.

No	Image analysis method	Name of disaster case	Type of disaster	Page number
1	Interferometric SAR analysis	Mount Hakone, Japan	Volcano	10
2	Superimposition of images with different polarized waves	Kumamoto Earthquake of 2016	Earthquake	13
3	Superimposition of images from different timings	Kanto/Tohoku Torrential Rains of September 2015	Flood/ Landslide	17
4		Typhoon No.9 (Mindulle) of 2016 (Tokoro River Hokkaido)		21

Disaster Case - 1 [Volcano]

2015 Mount Hakone

Volcanic earthquakes with epicenters at Owakudani increased from 26 April 2015, and on 6 May the volcanic alert was raised from level 1 (note that it is an active volcano) to level 2 (Do not approach the crater). Thus, Hakone Town issued evacuation instructions for the vicinity of Owakudani at 6:10 am of that day and restricted entry around the crater. Although the number of earthquakes tended to decrease in mid-June, volcanic earthquakes again increased from around 7:30 on 29 June, and volcanic tremors, the first to be comfirmed in the history of its observation, was also confirmed. On 30 June, a small pyroclastic hill was confirmed in Owakudani, and the volcanic alert was raised from level 2 to 3 (Do not approach the volcano). From late August, the crustal deformation indicating expansion of the mountain was considered to be slowing, and the volcanic alert was lowered to level 2 on 11 September.

On 4 May, volcanic activity of Mount Hakone increased and JAXA conducted emergency observation by ALOS-2 and provided observed data upon request from the “Satellite Data Analysis Group (Volcano WG)” (secretariat: Japan Meteorological Agency (JMA)) established under the Coordinating Committee for Prediction of Volcanic Eruptions. Results of analysis by the Volcano WG members Hot Springs Research Institute of Kanagawa Prefecture and the Geospatial Information Authority of Japan (GSI), were reported to Hakone Town and the Hakone Volcano Coordinating Committee, and was used for decision making of the re-opening of restricted areas and safety measures.

■Crustal deformation extraction

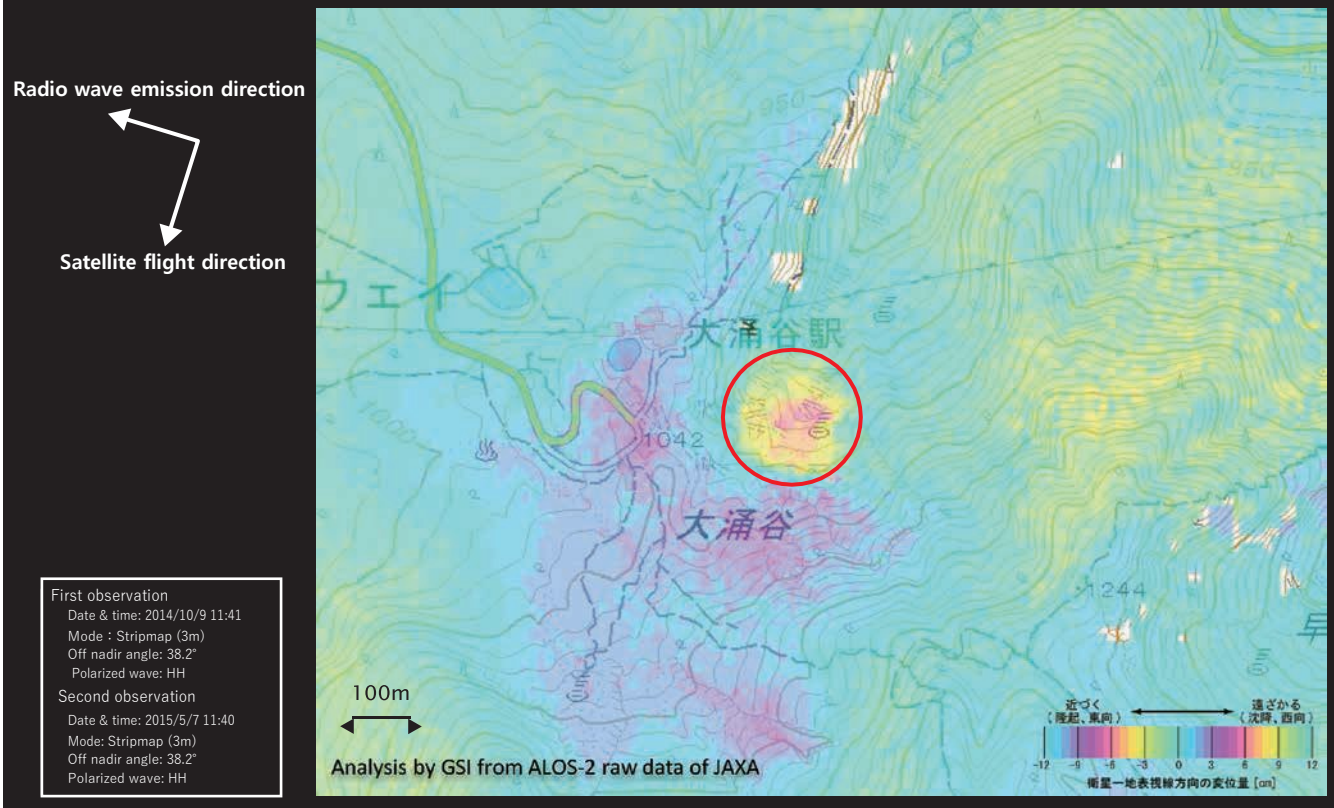

Fig. 1: Differential interferometry image (change between 9 Oct 2014 – 7 May 2015)
Shift towards the satellite of about maximum 6cm was observed within an extremely small area of 200m diameter in Owakudani. This shift could possibly have captured an expansion in a shallow place underground. The volcanic alert was raised from level 1 to 2 on 6 May 2015.

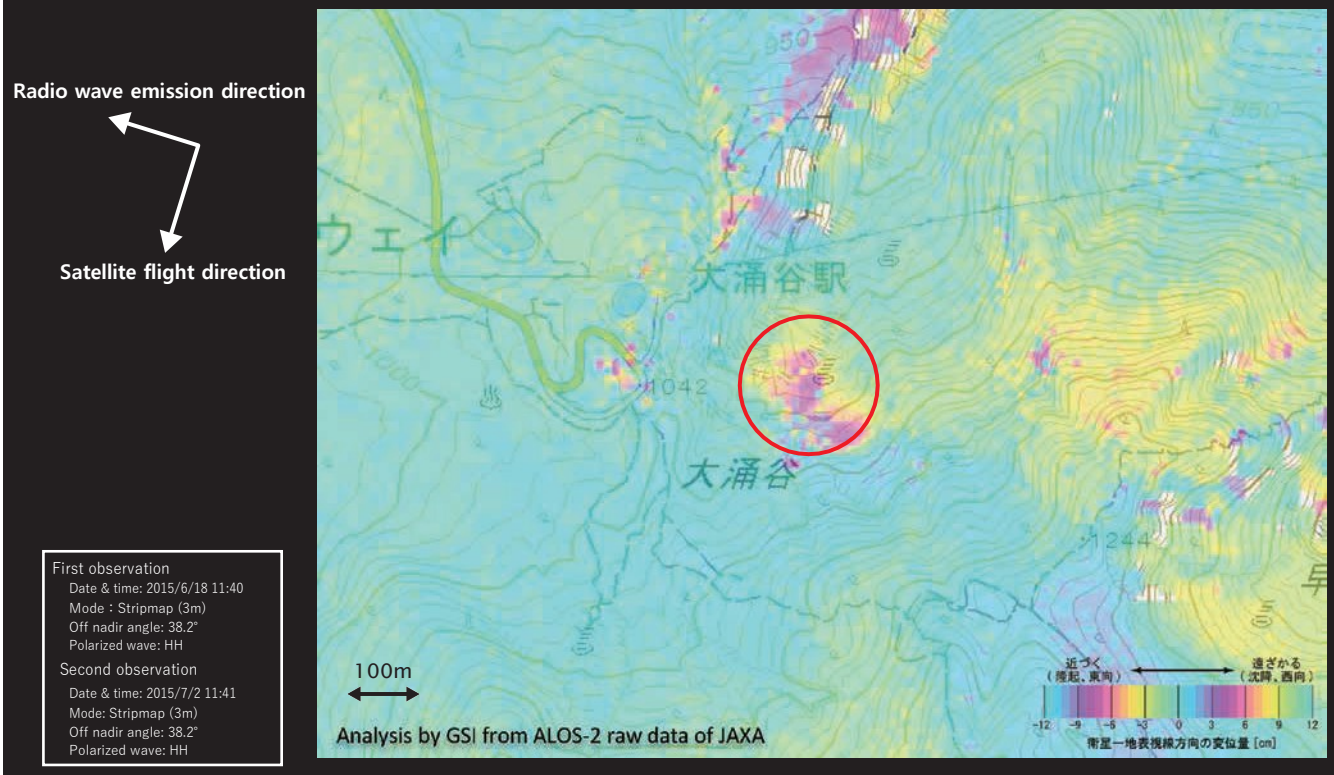

Fig.2: Differential interferometry image (change between 18 June – 2 July 2015)
No significant change in the range and distribution of amount of change is seen. In two weeks, crustal deformation of about maximum 10cm was observed. The volcanic alert was raised from level 2 to 3 on 30 June 2015.

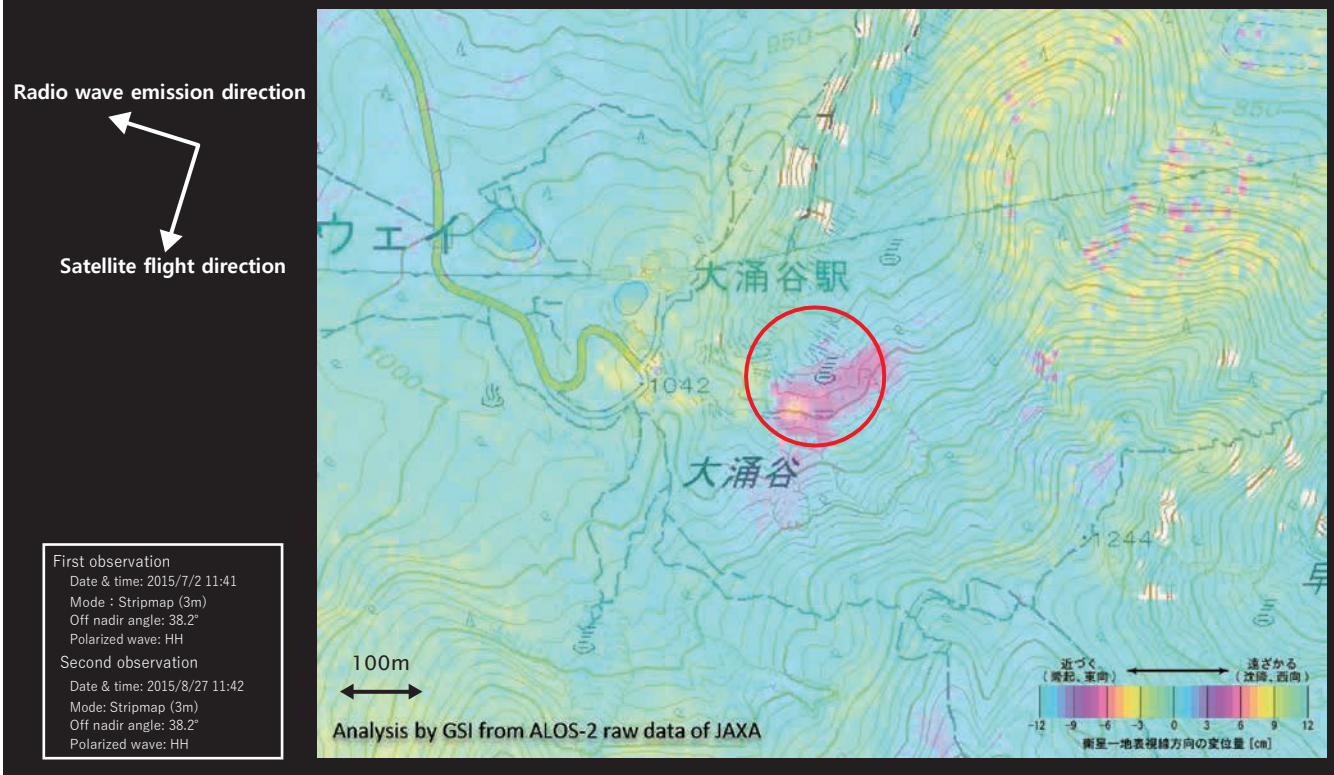

Fig. 3: Differential interferometry image (change between 2 July – 27 Aug 2015)
Around maximum 3cm shift away from the satellite was observed, although equivalent to noise level, in the area of fluctuation (red area). There is a possibility of shrinking fluctuation occurring following the small-scale eruption at the end of June.

Utilization at the Coordinating Committee for Prediction of Volcanic Eruptions

Interferometry analysis result using ALOS-2 observation data was utilized in the Japan Meteorological Agency (JMA)'s report at the 133rd Coordinating Committee for Prediction of Volcanic Eruptions held on 21 October 2015. It was said that it greatly contributed in volcanic activity evaluation and the JMA's volcanic alert level decisions.

Report document at the 133rd Coordinating Committee for Prediction of Volcanic Eruptions

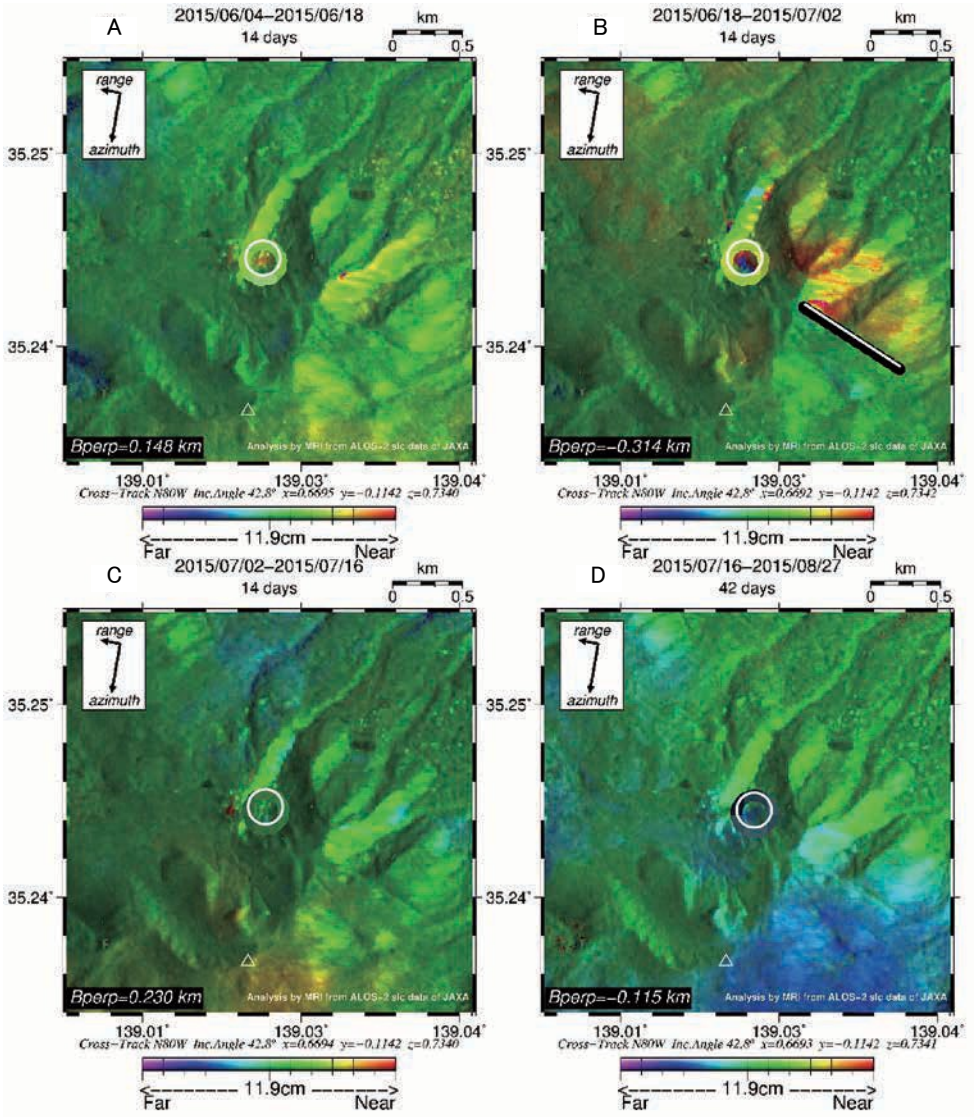

Fig. 4: Report at the 133rd Coordinating Committee for Prediction of Volcanic Eruptions
The position around Owakudani is indicated by the white circle, and the peak of Mount Hakone by the white triangle. Significant phase change can be observed around Owakudani in the pair before and after 29 June when the eruption occurred (Fig. B). Significant phase change is also observed in the area east to south-east of Owakudani, and abrupt phase change can be recognized in certain parts (white dotted line). (Excerpt from 133rd Coordinating Committee for Prediction of Volcanic Eruptions document)

Above left
- First observation
  - Date & time: 2015/6/4 11:43
  - Mode: Stripmap (3m)
  - Off nadir angel 38.2°
  - Polarized wave: HH
- Second observation
  - Date & time: 2015/6/18 11:40
  - Mode: Stripmap (3m)
  - Off nadir angel: 38.2°
  - Polarized wave: HH

Above right
- First observation
  - Date & time: 2015/6/18 11:40
  - Mode: Stripmap (3m)
  - Off nadir angle: 38.2°
  - Polarized wave: HH
- Second observation
  - Date & time: 2015/7/2 11:41
  - Mode: Stripmap (3m)
  - Off nadir angle: 38.2°
  - Polarized wave: HH

Below left
- First observation
  - Date & time: 2015/7/2 11:41
  - Mode: Stripmap (3m)
  - Off nadir angle: 38.2°
  - Polarized wave: HH
- Second observation
  - Date & time: 2015/7/16 11:43
  - Mode: Stripmap (3m)
  - Off nadir angle: 38.2°
  - Polarized wave: HH

Below right
- First observation
  - Date & time: 2015/7/16 11:43
  - Mode: Stripmap (3m)
  - Off nadir angle: 38.2°
  - Polarized wave: HH
- Second observation
  - Date & time: 2015/8/27 11:42
  - Mode: Stripmap (3m)
  - Off nadir angle: 38.2°
  - Polarized wave: HH

Disaster Case - 2 [Earthquake]

2016

Kumamoto Earthquake of 2016

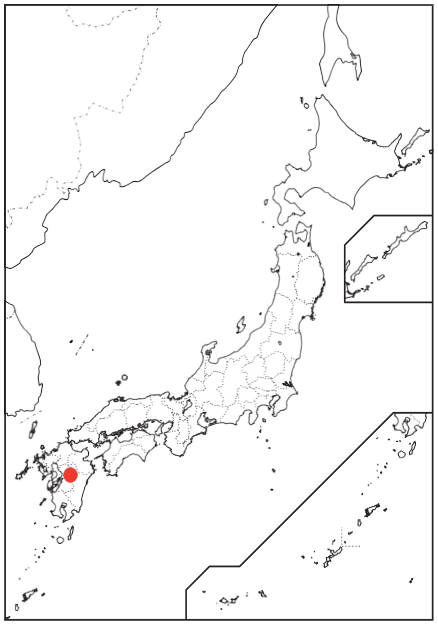

At 21:26 JST on 14 April 2016, an earthquake with a magnitude (Mj) of 6.5 occurred in the Kumamoto area of Kumamoto Prefecture, and observed seismic intensity of 7 in Mashiki Town and 6- in Tamana and Kumamoto Cities etc. Then, at 1:25 on 16 April, a larger earthquake of magnitude (Mj) 7.3 occurred with seismic origin in the same area, and observed seismic intensity of 7 in Mashiki Town and Nishihara Village, 6+ in Minamiaso village, Kikuchi City etc., and 6- to 1 from the Kyushu region to parts of the Tohoku region. This earthquake occurred in the crust, and is reported as a strike-slip fault type with a tension axis in the north-south direction. A series of seismic activities occurred in this area between the two earthquakes and those with seismic intensity of 1 or more occurred 4,068 times by 30 September. These earthquake activities caused damage of 8,204 houses totally destroyed, 30,390 houses half destroyed, 139,320 houses partly damaged, 15 fires etc. (as of 30 September).

On 14 April 2016 following disaster occurrence, JAXA conducted emergency observation and provided observed data upon request from the “Earthquake SAR Analysis Working Group (Earthquake WG)” (secretariat: Geospatial Information Authority of Japan (GSI)) established under the Coordinating Committee for Earthquake Prediction. Crustal deformation was observed from differential interferometry results of image observed by ALOS-2, and used on the GSI’s website and in the report to the Earthquake Research Committee (special meeting) (17 April 2016).

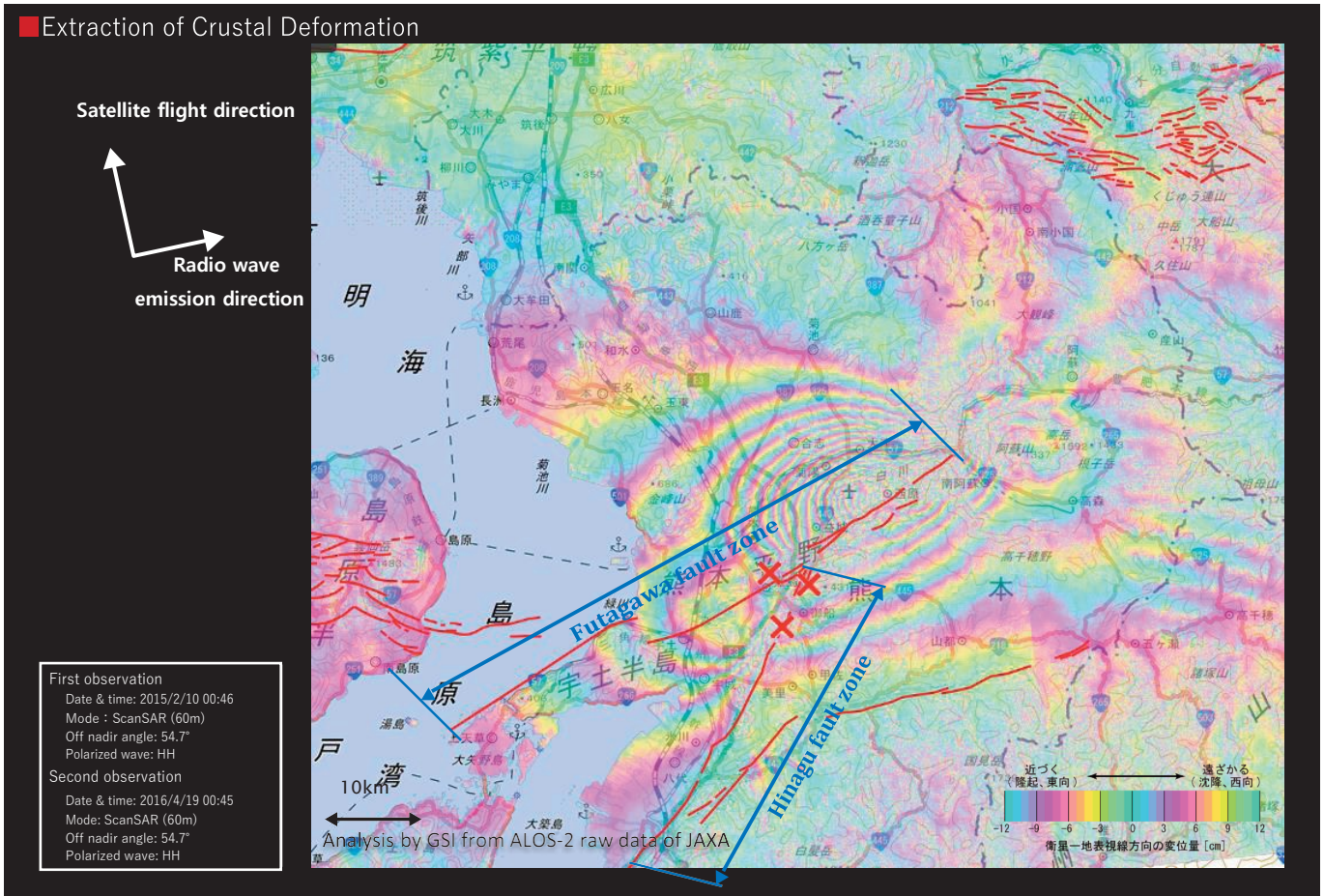

Fig.1: Differential interferometry image (change between 10 February 2015 – 19 April 2016)
On the north side of the Futagawa fault zone, sinking and eastward shift of up to 1 m or more, and on the south side uplift of up to 30 cm and westward shift of 50 cm or more can be seen. On the Hinagu fault zone, eastward shift on the northwest side and westward shift on the southeast side can be seen, although on a smaller scale.

Utilization in 2.5-Dimensional Analysis by GSI

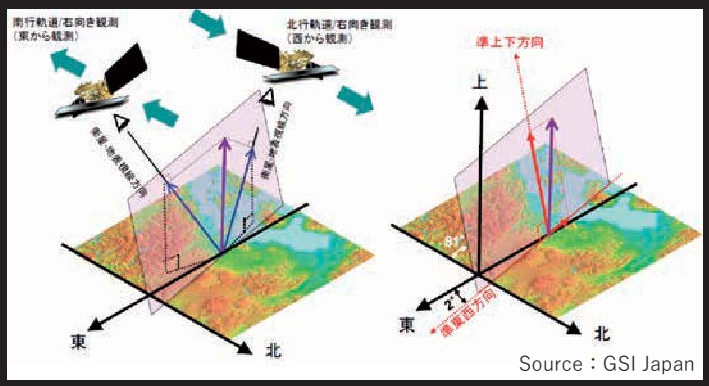

Fig. 2: Principle of 2.5-dimensional analysis using interferometric SAR image
It is possible to estimate the change value (purple arrow) of the two dimensions (pink plane) from the easterly and westerly observation results (blue arrow), and separate it into the quasi-vertical component and the quasi-east-west component (red arrow). This analysis method is called 2.5-dimensional analysis by GSI.
For details please see the GSI homepage below;
http://www.gsi.go.jp/BOUSAI/H27-kumamoto-earthquake-index.html

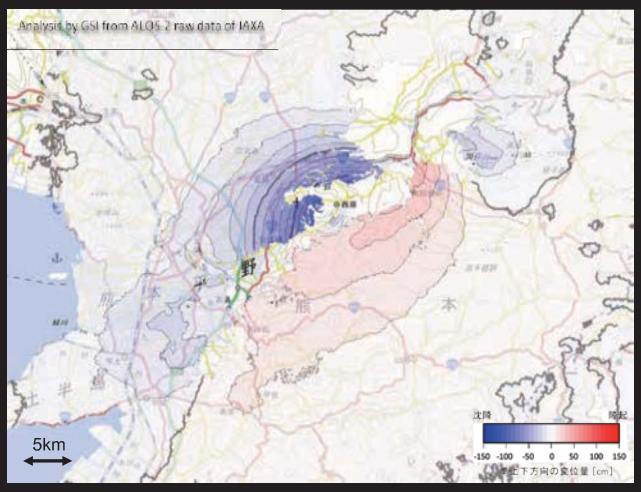

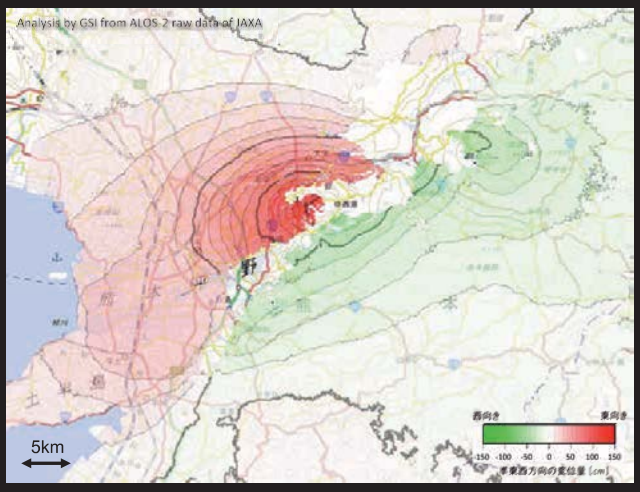

Fig. 3: 2.5-dimensional analysis using interferometric SAR image (left: change in vertical component, right: change in east-west component) GSI Japan combined the results of interferometric SAR images (7 March 2016 - 18 April 2016, 10 February 2015 - 19 April 2016), conducted 2.5-dimensional analysis and elucidated the quasi-vertical component and quasi-east-west component of the crustal deformation.

Descending orbit/right-side observation
First observation
Date & time: 2016/3/7 12:17
Mode: Stripmap (3m)
Off nadir Angle: 32.4°
Polarized wave: HH
Second observation
Date & time: 2016/4/18 12:17
Mode: Stripmap (3m)
Off nadir angle: 32.4°
Polarized wave: HH

Ascending orbit/right-side observation
First observation
Date & time: 2015/2/10 00:46
Mode: ScanSAR (60m)
Off nadir angle: 54.7°
Polarized wave: HH
Second observation
Date & time: 2016/4/19 00:45
Mode: ScanSAR (60m)
Off nadir angle: 54.7°
Polarized wave: HH

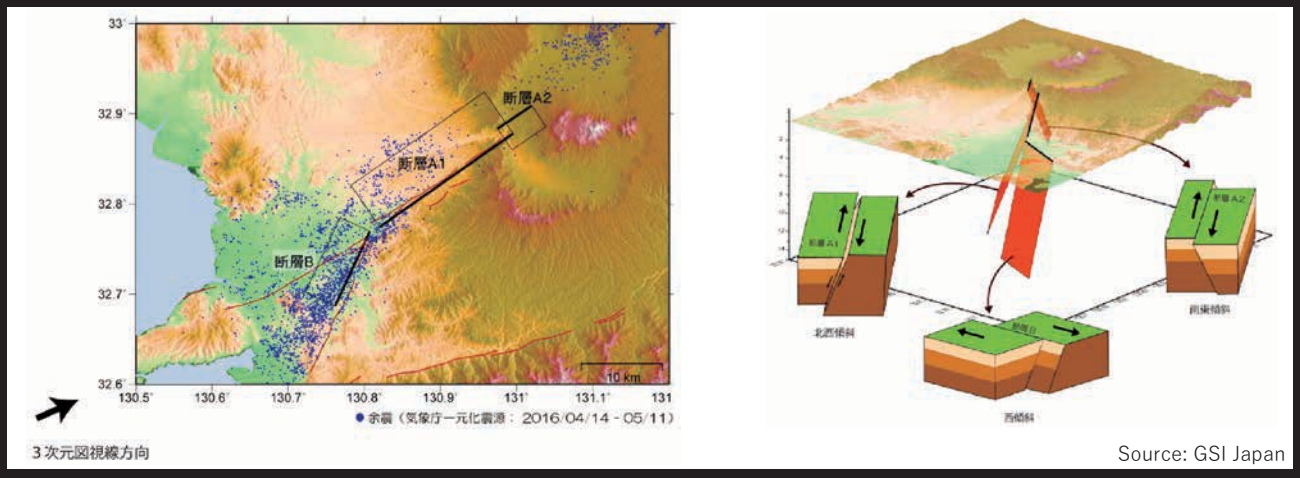

Fig. 4: Utilization in the Kumamoto earthquake epicenter fault model (interim version)
2.5-dimensional analysis using ALOS-2 image and change in GNSS-based control stations were analyzed, and utilized in the Kumamoto earthquake epicenter fault model (interim version).

Landslide site near the Great Aso Bridge

Before disaster

After disaster

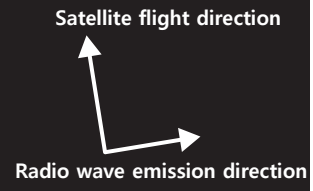

Observation before disaster
Date & time: 2 015/12/4 00: 11
Mode: Stripmap (6m)
Off nadir angle: 30.4°
Polarized wave: HH+HV+VH+VV
Observation after disaster
Date & time: 2016/4/22 00:11
Mode: Stripmap (6m)
Off nadir angle: 30.4°
Polarized wave: HH+HV+VH+ VV

Fig. 5: Polarized wave superimposed images of before and after the disaster (change between 4 Dec 2015-22 Apr 2016)
In the yellow outline part near the Great Aso Bridge, it was covered in green before disaster, while it has changed to purple synthesized from red and blue after the disaster. This shows that the HV image which responds brightly to forests became darker after the disaster, and it can be estimated that there was landslide in part of the forest. Refer to Fig. A.

Red, blue: HH polarized wave
Green: HV polarized wave

Fig. A: Difference between Polarization HH and HV for land texture

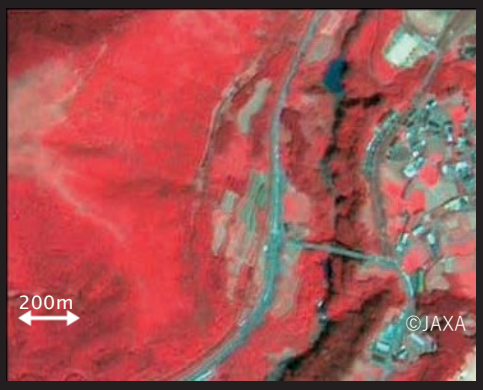

Before disaster

After disaster

Observation before disaster
(ALOS PRISM/AVNIR-2 pansharpened)
Date & time: 2011/4/6 11:02
Resolution: 2.5m
Observation after disaster
(SPOT-6 pansharpened)
Date & time: 2016/4/16 10:38
Resolution: 1.5m

Fig. 6: False-color image before and after disaster (change between 6 April 2011 – 17 April 2016)
In the false-color image, vegetation responds brightly to near infrared image and appears red. Where it was covered in red before the disaster, is recognized to have changed brown with the landslide location after the disaster.

Red: near infrared wavelength
Green: red wavelength
Blue: green wavelength

Photo 1: Vicinity of the Great Aso bridge after disaster (aerial photo) (16 Apr 2016)

Photo 2: Vicinity of the Great Aso bridge after disaster (2 May 2016)

Landslide site near Kyoto University Volcanological Laboratory

Before disaster

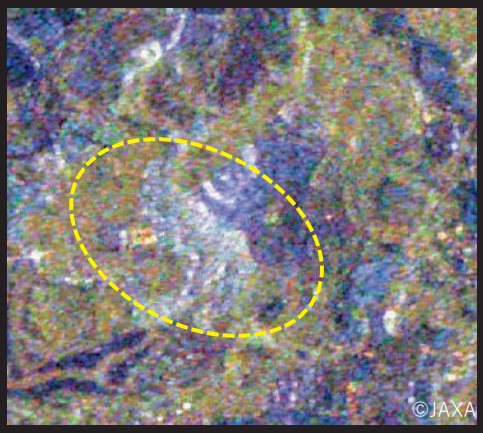

After disaster

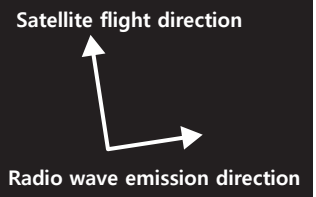

Observation before disaster
Date & time: 2015/12/4 00:11
Mode: Stripmap (6m)
Off nadir angle: 30.4°
Polarized wave: HH+HV+VH+VV
Observation after disaster
Date & time: 2016/4/22 00:11
Mode: Stripmap (6m)
Off nadir angle: 30.4°
Polarized wave: HH+HV+VH+VV

Fig. 7: Polarized wave superimposed images before and after the disaster (change between 4 Dec 2015 – 22 Apr 2016)
In the yellow outline part near the Kyoto University Volcanological Laboratory, it was covered in green before disaster, while it has changed to purple synthesized from red and blue after the disaster. This shows that the HV image which responds brightly to forests became darker after the disaster, and it can be estimated that there was landslide in part of the forest.
Red, blue: HH polarized wave
Green: HV polarized wave

Before disaster

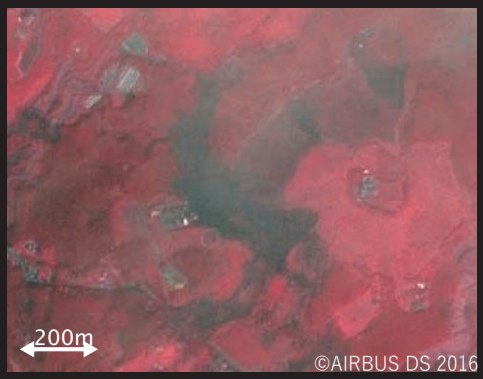

After disaster

Observation before disaster
(ALOS PRISM/AVNIR-2 pansharpened)
Date & time: 2011/4/6 11:02
Resolution: 2.5m
Observation after disaster
(SPOT-6 pansharpened)
Date &time: 2016/4/16 10:38
Resolution: 1.5m

Fig. 8 False-color image before and after disaster (change between 6 Apr 2011 – 17 Apr 2016)
In the false-color image, vegetation responds brightly to near infrared image and appears red. Where it was covered in red before the disaster, is recognized to have changed brown with the landslide location after the disaster.

Red: Near infrared wavelength
Green: Red wavelength
Blue: Green wavelength

Photo 3: Vicinity of the Kyoto University Volcanological Laboratory after disaster (aerial photo) (16 Apr 2016)

Photo 4: Vicinity of the Kyoto University Volcanological Laboratory after disaster (2 May 2016)

Disaster Case - 3 [Floods]

2015

Kanto/Tohoku Torrential Rains of September 2015

In September 2015, southerly moist winds flowing toward a low pressure originally Typhoon No. 18 and the moist winds flowing from Typhoon No. 17 moving northward over the east sea of Japan produced many linear rainwater bands in succession and record rainfall was observed in the Kanto and Tohoku regions. Particularly, from 9 to 11 September, the maximum 24 hours rainfall at 16 observation points with more than 10 years of recording reached the highest, such as Nikko and Imaichi Cities in Tochigi, Koga City in Ibaraki and Mt. Izumigatake of Sendai City in Miyagi Prefectures. Flooding damages occurred in Tochigi, Ibaraki and Saitama Prefectures and the Kinugawa River flowing through Tochigi and Ibaraki Prefectures caused catastrophic damages such as the embankment destruction in Joso City.

Extraction of estimated flooded areas

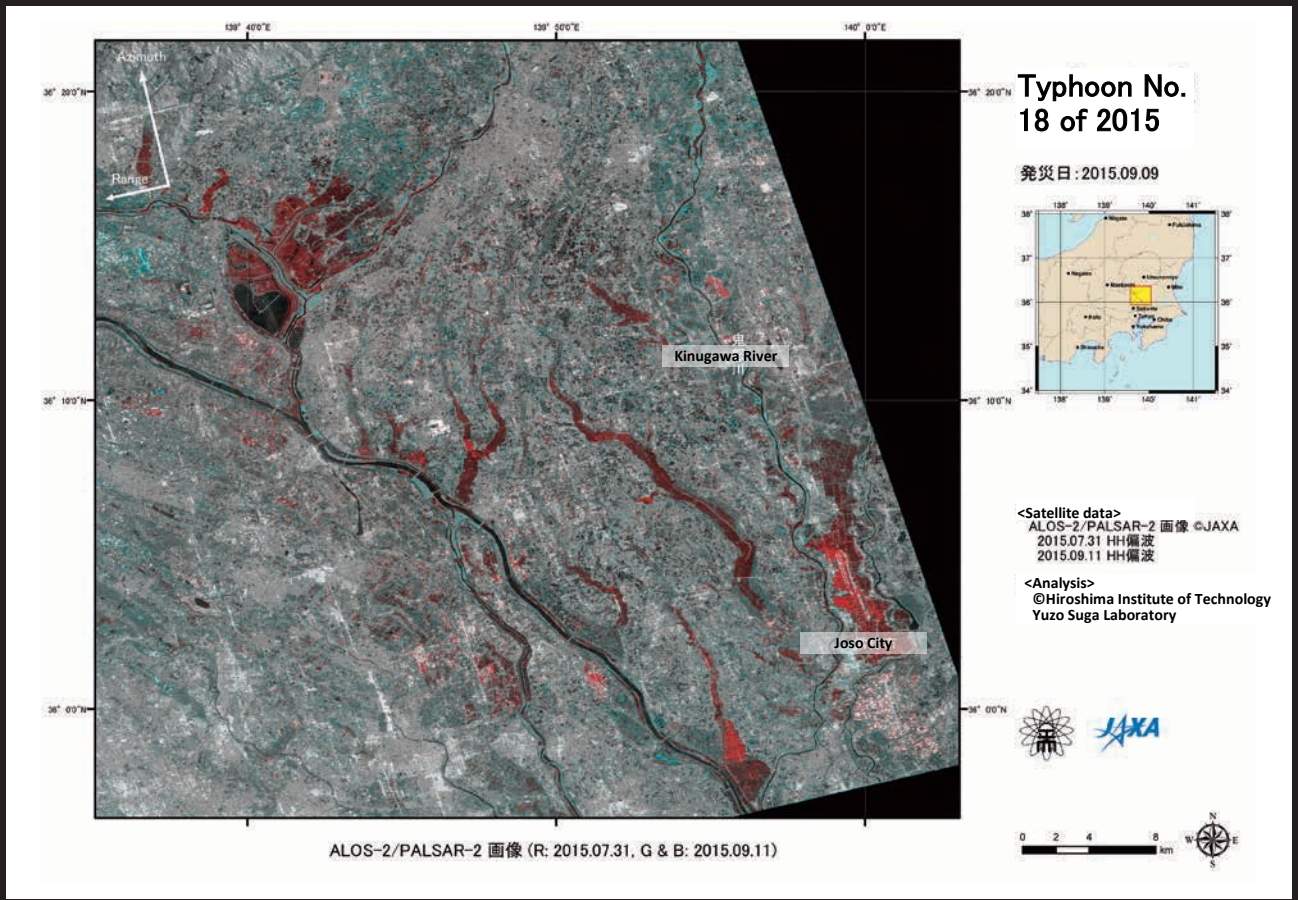

Fig. 1: Estimated flooded area extraction image by ALOS-2
An analysis example of flooded area estimation from images before and after disaster. Red is assigned to the pre-disaster image of 31 Jul 2015, and blue and green to the post-disaster image of 11 Sep 2015. In this result, the red estimated flooded area is extracted.

Red: 31 July 2015
Blue, green: 11 September 2015

Observation before disaster
Date & time: 2015/7/31 22:56
Mode: Stripmap (3m)
Off nadir angle: 35.4°
Polarized wave: HH
Observation after disaster
Date & time: 2015/9/11 22:56
Mode: Stripmap (3m)
Off nadir angle: 35.4°
Polarized wave: HH

Upon request from the Ministry of Land, Infrastructure, Transport and Tourism (MLIT), JAXA conducted emergency observation and provided analyzed data such as estimated flooded area extraction to disaster mitigation agencies. MLIT considered ALOS-2 analyzed image together with optical satellite imagery and aerial photos, and grasped post-bank-rip flooded area of Kinugawa River and conducted deployment and operation of water pump vehicles.

■Flooded area around Joso City

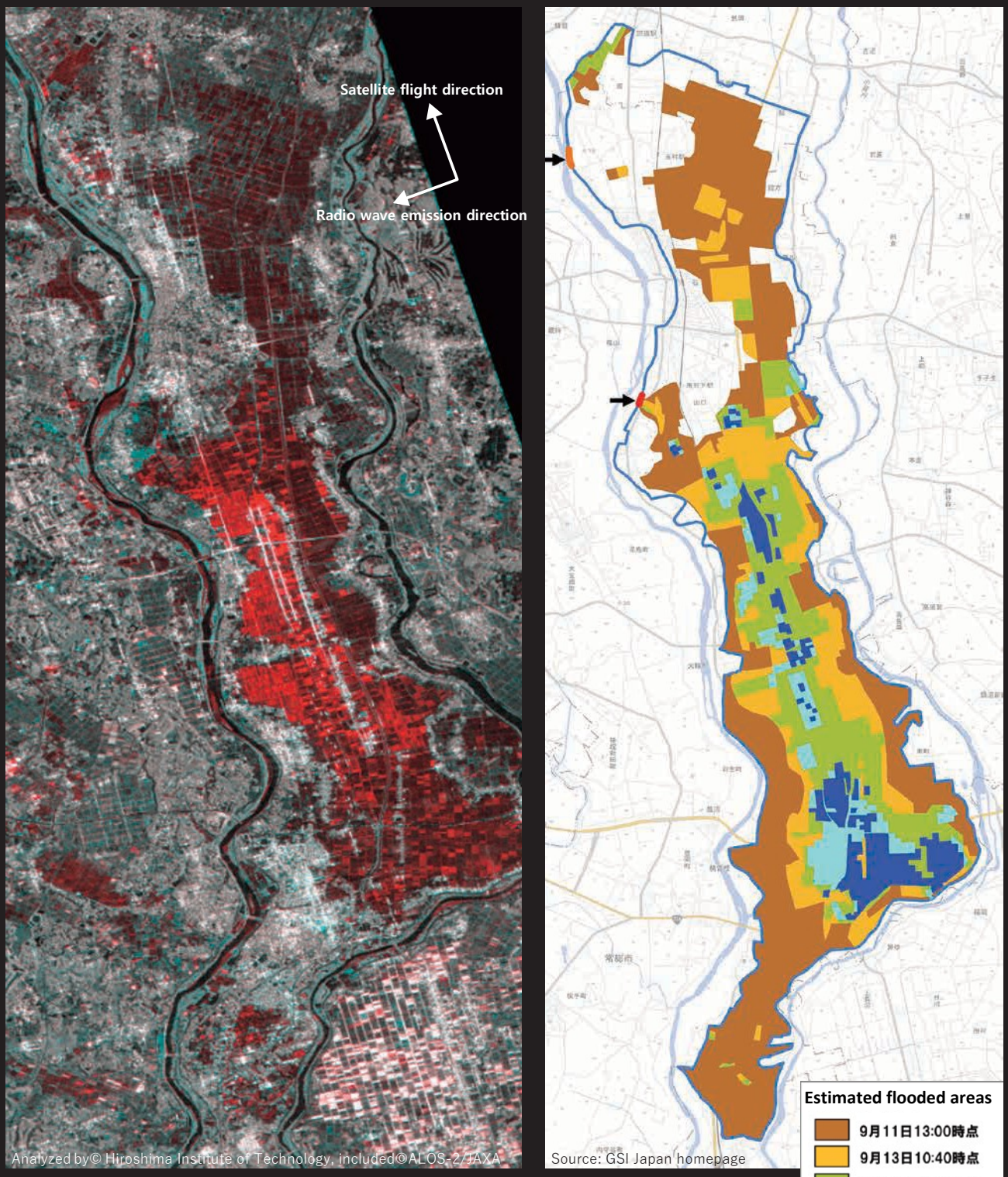

Fig. 2: ：Estimated flooded area extraction image by ALOS-2
(Left: enlargement of Fig. 1 Joso City, right: estimated flooded area up to 16 Sep 2015)
The area of Joso City which suffered catastrophic flooding due to embankment destruction is shown enlarged in Fig. 2. It can be seen that the results are similar to the Geospatial Information Authority of Japan (GSI)'s estimated flooded area of 11 Sep 13:00 (brown). It is possible to obtain such analysis results regularly by SAR satellites such as ALOS-2 regardless of day/night or weather conditions.

Grasping the infrastructures damage situation upon disaster

With ALOS-2, it is also possible to grasp the damage situation of infrastructures using 3m resolution Stripmap mode. The following are analysis examples concerning some infrastructures which suffered damage in this flooding.

Utsunomiya City, Higashiosakabe-machi vicinity

Before disaster

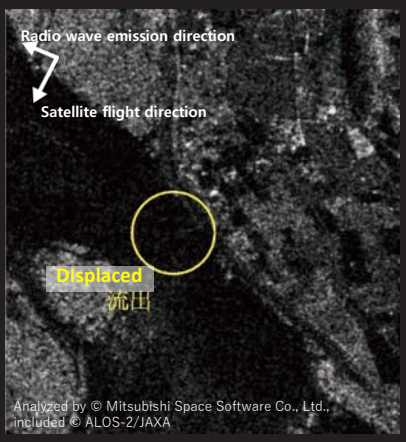

After disaster

Observation before disaster
Date & time: 2015/8/13 11:42
Mode: Stripmap (3m)
Off nadir angle: 35.4°
Polarized wave: HH
Observation after disaster
Date & time: 2015/9/10 11:42
Mode: Stripmap (3m)
Off nadir angle: 35.4°
Polarized wave: HH

Fig. 3: Outflow of diving bridge at Higashiosakabe-machi, Utsunomiya City, Tochigi Prefecture
Analysis result of diving bridge displacement. The bridge cannot be recognized in the post-disaster image with the possibility of its outflow.

Photo1: Diving bridge (1 Oct 2015 around 11:00 a.m.)

Joso City Wakamiyado vicinity

Before disaster

After disaster

Observation before disaster
Date & time: 2015/8/13 11:42
Mode: Stripmap (3m)
Off nadir angle: 35.4°
Polarized wave: HH
Observation after disaster
Date & time: 2015/9/10 11:42
Mode: Stripmap (3m)
Off nadir angle: 35.4°
Polarized wave: HH

Fig. 4: Embankment overflow at Wakamiyado in Joso City, Ibaraki Prefecture
Analysis result of embankment overflow (10 Sep after 6 a.m.). Embankment overflow can be extracted from the post-disaster image.

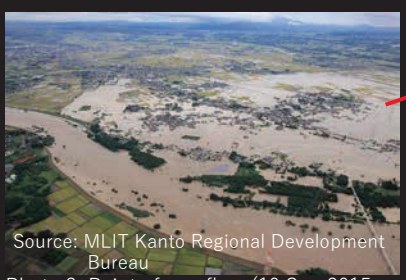

Photo 2: Point of overflow (10 Sep 2015 around 15:00)

Joso City Misaka-machi vicinity

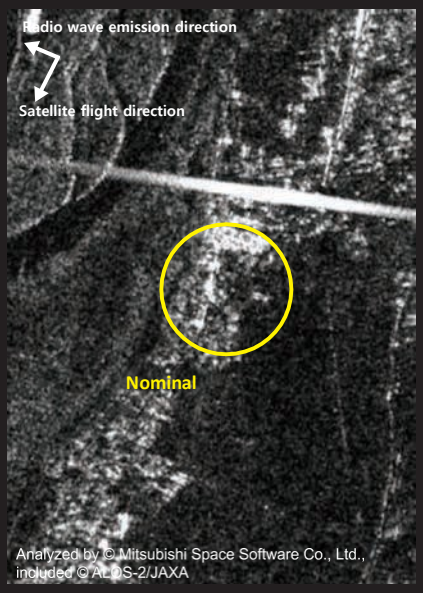

Before disaster 1

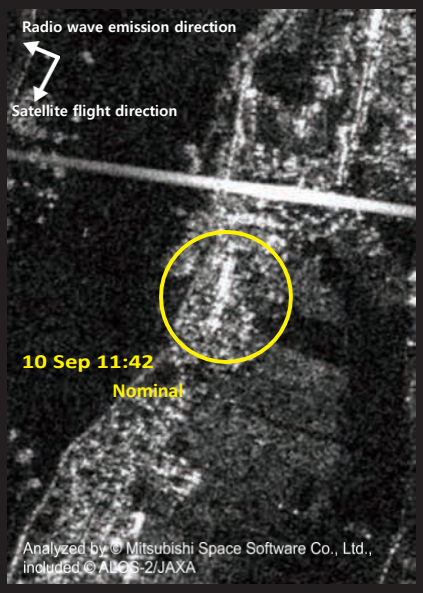

Before disaster 2

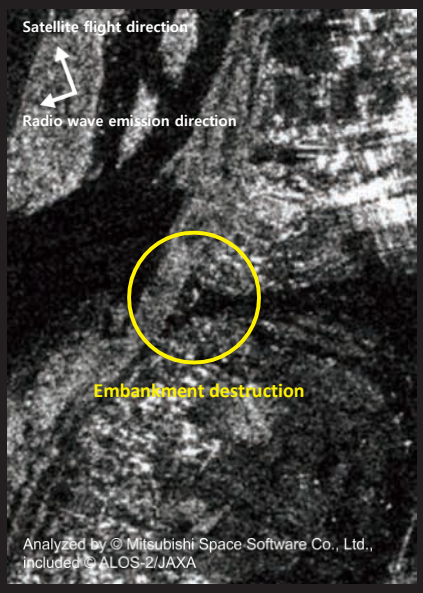

After disaster

Observation before disaster 1
Date & time: 2015/8/13 11:42
Mode: Stripmap (3m)
Off nadir angle 35.4°
Polarized wave: HH
Observation before disaster 2
Date & time: 2015/9/10 11:42
Mode: Stripmap (3m)
Off nadir angle: 35.4°
Polarized wave: HH
Observation after disaster
Date & time: 2015/9/11 22:56
Mode: Stripmap (3m)
Off nadir angle: 35.4°
Polarized wave: HH

Photo 3: Point of embankment destruction
(10 Sep 2015 around 15:00)

Photo 4: Point of embankment destruction
(10 Sep 2015 around 15:00)

Fig. 5: Embankment destruction at Misaka-machi in Joso City, Ibaraki Prefecture (10 September, 12:50)
Monitoring result of embankment destruction at Misaka-machi. Embankment destruction can be extracted in the post-disaster image. As the observation direction is different in the post-disaster image, it is necessary to note that the appearance is different. In this case, it is deemed to be an embankment destruction as the vicinity of the yellow circle has darkened markedly.

Disaster Case - 4 [Floods]

2016

Typhoon No.9 (Mindulle) of 2016

(Tokoro River, Hokkaido)

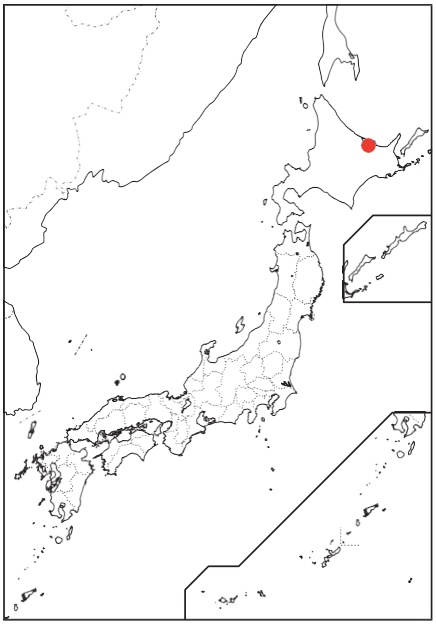

Typhoon No.9 (Mindulle) which formed in the Mariana Islands on 19 August 2016, grew and moved north in the south of Japan, and made landfall at around 12:30 on 22 August near Tateyama City, Chiba Prefecture. It then crossed the Kanto/Tohoku regions accelerating and made landfall again at around 6:00 on 23 August in the Hidaka region of Hokkaido. Due to the lingering fronts and approaching and passing of successive typhoons, record heavy rain was observed in a wide area and total rainfall from 20 to 23 August was 296.0mm at Itokushibetsu in Nemuro region, 291.5mm in Rausu and Hidaka-monbetsu of Hidaka region. Due to heavy rain, many rivers flooded, including the Tokoro River on the Sea of Okhotsk side, causing damage such as above/below floor level inundation of houses. Landslides occurred in various places, and partial damage to homes were also caused. Evacuation instructions and recommendations were issued for several days in many cities, towns and villages for fear of floods and landslides, and traffic interruption of national highways and roadways and service suspension of Japan Railway (JR) occurred. Together with Typhoon No. 7, which landed near Erimo Cape on 17 August and Typhoon No. 11, which landed near Kushiro City on 21 August, three typhoons landed in Hokkaido in a week.

With the overflow of Tokoro River in Hokkaido at 0:40 on 21 August 2016, JAXA received ALOS-2 emergency observation request from the River Planning Division of the Ministry of Land, Infrastructure, Transport and Tourism (MLIT). Although observation on 21 August was withheld as conditions were not satisfactory for both day and night passes, ALOS-2 day and night pass observation was conducted upon request on 22 August when flooding increased in the same river, since investigation by helicopter etc. was difficult due to bad weather, and image product was provided. Automatic analysis for disaster maps together with flooding area extraction polygon by manual interpretation were provided and, under cooperation with the Geospatial Information Authority of Japan (GSI), shared information with the Hokkaido Regional Development Bureau via MLIT's Integrated Disaster Information Mapping System (DiMAPS). Also, estimation of flooding volume was conducted by GSI Japan using DEM (5m mesh).

Characteristics of Typhoon No.9 and 10 of 2016

(1) First in observation history (3 typhoons to make landfall in Hokkaido in a year, first to make landfall in Tohoku region from the Pacific Ocean side)
(2) First flood disaster since the Kanto/Tohoku Torrential Rain of September 2015 after MLIT expanded ALOS-2 utilization in flood disasters
(3) Large scale flood and landslide disaster, occurring numerously and simultaneously all over Hokkaido, Tohoku region, etc.
(4) Bad weather conditions persisted and observation by helicopters etc. delayed. Not observable by commercial optical satellites

ALOS-2 observation and provided products, timeline

(1) Conducted emergency observation mainly of flood disaster locations, upon request from MLIT River Planning Division
(2) Conducted observation in the night of 30 August for landslide disaster inspection immediately after Typhoon No.10 passed Tohoku region, upon request from MLIT River Planning Division

Observation date	Observation time	Products provided		Observation area	
		Automatic analysis for disaster map (provision time) *nominal: observation +2 hours	Interpreted polygon/Analysis result (provision time) *nominal: observation +5 hours		
2016/8/22 (Mon)	12:15	(15:26)	(16:46)	Hokkaido	Tokoro River
2016/8/22 (Mon)	23:11	(01:26)	-	Hokkaido	Tokoro River
2016/8/23 (Tue)	12:35	(14:06)	(15:38)	Hokkaido	Bebetsu River (Ishikari River system)
2016/8/23 (Tue)	23:32	(00:14)	-	Hokkaido	Ishikari River
2016/8/30 (Tue)	11:48	(15:06)	-	Hokkaido	Coastal Akita Prefecture
2016/8/30 (Tue)	22:43	(00:43)	(next day 5:24)	Hokkaido	Coastal Iwate Prefecture
2016/8/31 (Wed)	12:08	(14:03)	-	Hokkaido	Tokachi River
2016/8/31 (Wed)	23:04	(23:53)	(08:56)	Hokkaido	Tokachi River
2016/9/1 (Thu)	12:28	(14:34)	(17:31)	Hokkaido	Sorachi River (Ishikari River system)
2016/9/1 (Thu)	12:28	(14:34)	(17:31)	Iwate Pref.	Omoto River
2016/9/1 (Thu)	23:24	(11:29)	(14:07)	Iwate Pref.	Kuji River
2016/9/1 (Thu)	23:24	(11:29)	(14:07)	Hokkaido	Satsunai River (Tokachi River system)

Extraction of flooded areas

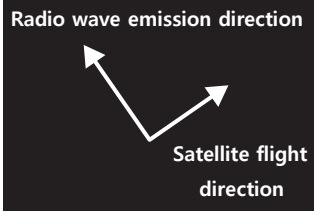

Observation before disaster
Date & time: 2014/12/1 12:14
Mode: Stripmap (3m)
Off nadir angle: 32.4°
Polarized wave: HH
Observation after disaster
Date & time: 2016/8/22 12:14
Mode: Stripmap (3m)
Off nadir angle: 32.4°
Polarized wave: HH

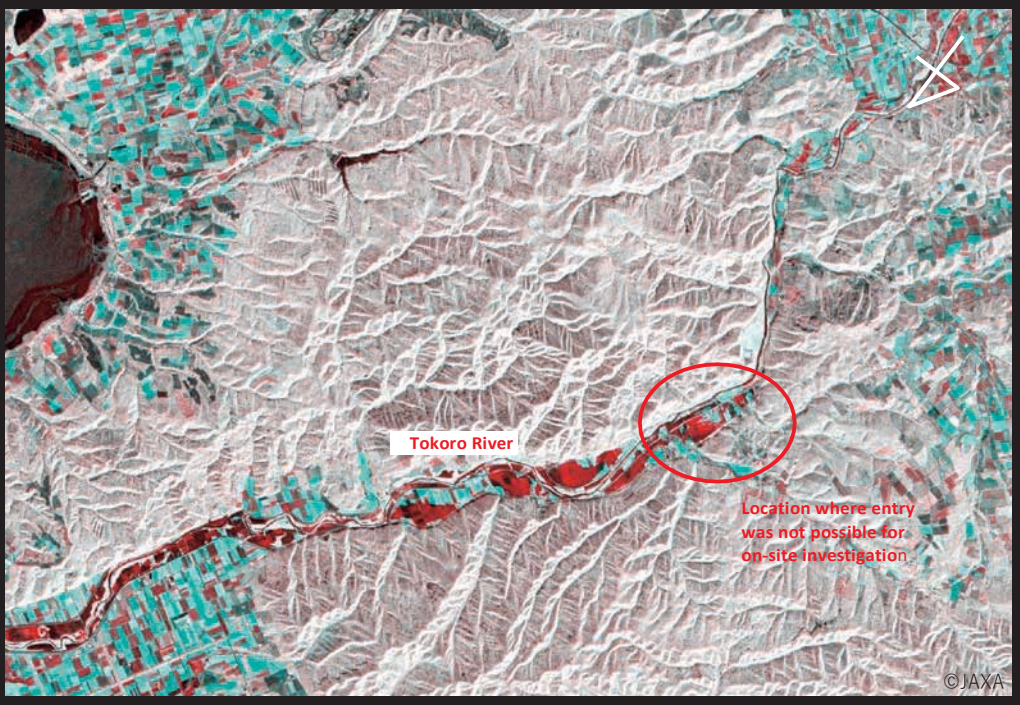

Flooded area extraction image near Tokoro River
Red: 1 December 2014
Green, blue: 22 August 2016

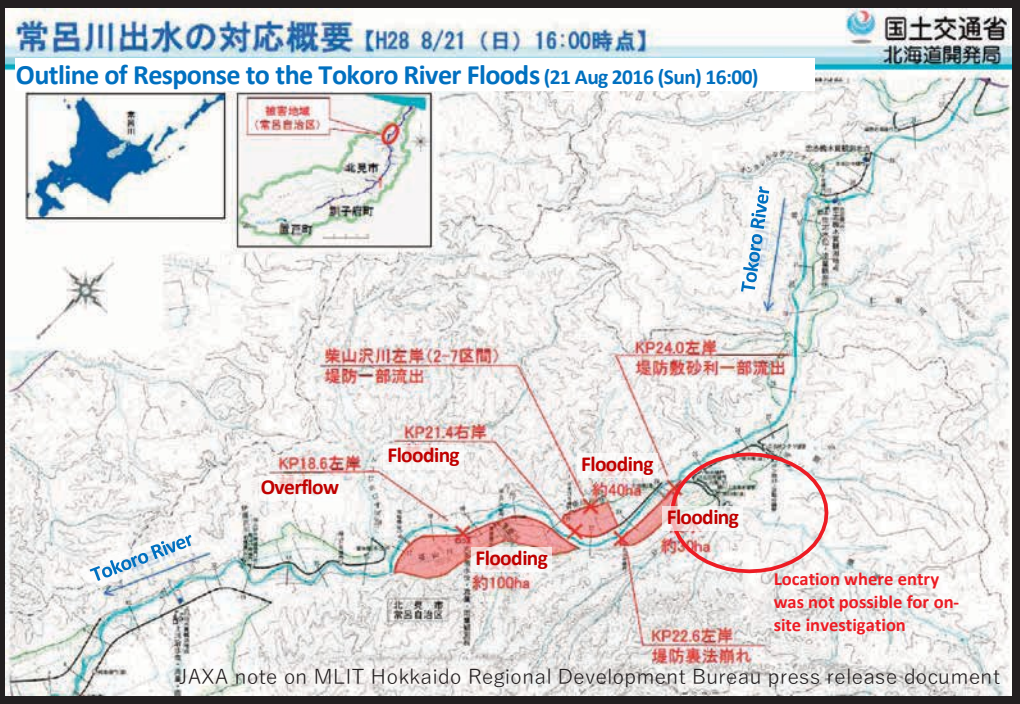

Flooded area map by the Hokkaido Regional Development Bureau (21 August 2016)

Fig. 1: Flooded area extraction image by ALOS-2 (above: flooded area extraction image near Tokoro River, below: flooded area map by the Hokkaido Regional Development Bureau)

Compared to the Hokkaido Regional Development Bureau's flooded area map of 21 August 2016 16:00 based on on-site investigation, it can be observed from ALOS-2 observation of 22 August 12:00 how the flooded area is changing. It can be seen that ALOS-2 has extracted flooding in upstream areas where entry was not possible in the on-site investigation of 21 August 16:00. The flooded area extraction results from constant and night time ALOS-2 observation data was evaluated by the Hokkaido Regional Development Bureau as fully fit to be utilized.

List of Sources

●The sources of figures and photographs used in this document are as follows:

No	Item	Page	Figure, Photo	Source
1	Overview of Image Analysis	8	Fig. 9	Processed by Mitsubishi Space Software Co., Ltd. based on Geospatial Information Authority of Japan (GSI) homepage http://www.gsi.go.jp/common/000095940.pdf
2	Case 1 (Mount Hakone)	10, 11	Fig. 1, 2, 3	GSI Japan homepage http://www.gsi.go.jp/kikakuchousei/bousaichousei/h27-hakoneyama-index. html
		12	Fig. 4	Japan Meteorological Agency 133rd Coordinating Committee for Prediction of Volcanic Eruptions document http://www.data.jma.go.jp/svd/vois/data/tokyo/STOCK/kaisetsu/CCPVE/shiryo/133/133_04.pdf
3	Case 2 (Kumamoto Earthquake of 2016)	13, 14 15 16	Fig. 1, 3 Photo 1 Photo 3	GSI Japan homepage http://www.gsi.go.jp/BOUSAI/H27-kumamoto-earthquake-index.html
		14	Fig. 2	GSI Japan homepage http://www.gsi.go.jp/common/000139926.pdf
		14	Fig. 4	GSI Japan homepage http://www.gsi.go.jp/common/000140781.pdf
4	Case 3 (Kanto/Tohoku Torrential Rains of September 2015)	18	Fig. 2 (right)	GSI Japan homepage http://www.gsi.go.jp/common/000107669.pdf
		19, 20	Fig. 3, 4, 5 (map)	GSI Japan homepage http://maps.gsi.go.jp/
		19, 20	Photo 2, 3, 4	Ministry of Land, Infrastructure, Transport and Tourism (MLIT), Kanto Regional Development Bureau homepage http://www.ktr.mlit.go.jp/bousai/index00000047.html (the photographs are no longer on the above homepage)
5	Case 4 (Typhoon No.9 (Mindulle) of 2016) (Tokoro River Hokkaido)	22	Fig. 1 (below)	MLIT, Hokkaido Regional Development Bureau document https://www.hkd.mlit.go.jp/ky/saigai/press_h2808/21_houdou09.pdf

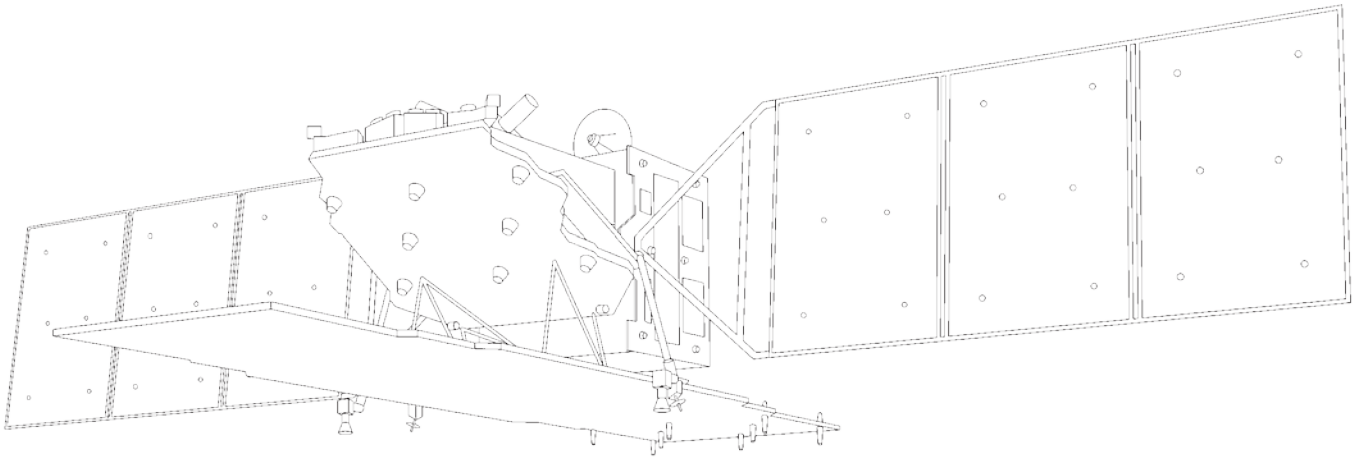

Space Application for Disaster Monitoring

- Collection of Good Practice in Disaster Emergency Observation by ALOS-2 “DAICHI 2” from 2014 to 2017 -
(Excerpts)

First published in Japanese in March 2018
Excerpts translated into English in July 2018
Japan Aerospace Exploration Agency (JAXA)
Satellite Applications and Operations Center (SAOC)

Japanese version editing assistance
Mitsubishi Space Software Co., Ltd.
Mitsubishi Electric Co., Ltd.

For questions concerning ALOS-2 utilization please contact
Satellite Applications and Operations Center
Space Technology Directorate I
Japan Aerospace Exploration Agency
Ochanomizu sola city 4-6 Kandasurugadai, Chiyoda-ku, Tokyo
101-8008 Japan
E-mail: sapc-info@ml.jaxa.jp